Ravelo Ana Christina (Orcid ID: 0000-0003-3929-677X)
Dang Haowen (Orcid ID: 0000-0002-1320-4761)
Jian Zhimin (Orcid ID: 0000-0002-2037-3539)

Nitrogen isotope variations in the northern South China Sea since marine isotopic stage 3: reconstructed from foraminifera-bound and bulk sedimentary nitrogen

Tingting Wang[1], Ana Christina Ravelo[2], Haojia Ren[3], Haowen Dang[1], Haiyan Jin[1], Jingjing Liu[1], and Zhimin Jian[1,*]

1. State Key Laboratory of Marine Geology, Tongji University, Shanghai
2. Ocean Sciences Department, University of California, Santa Cruz, CA
3. Department of Geosciences, National Taiwan University, Taipei

* Corresponding author: Zhimin Jian (jian@tongji.edu.cn)

Key Points:

- Terrigenous input affects $\delta^{15}N_{bulk}$ all over the South China Sea and can strongly obscure the $\delta^{15}N$ signal of the surface water
- Vertical mixing also plays a role on the general pattern of foraminifera-bound $\delta^{15}N$ in addition to nitrogen fixation in the SCS
- Foraminifera-bound $\delta^{15}N$ of *O. universa* have higher values than *G. ruber* and *G. sacculifer* due to its deeper habitat depth

This is the author manuscript accepted for publication and has undergone full peer review but has not been through the copyediting, typesetting, pagination and proofreading process, which may lead to differences between this version and the Version of Record. Please cite this article as doi: 10.1029/2018PA003344

Abstract

We report the differences between $\delta^{15}N$ of organic nitrogen bound in foraminifera tests (foraminifera-bound $\delta^{15}N$, or FB-$\delta^{15}N$), which is considered an effective recorder of thermocline nitrate $\delta^{15}N$ in the oligotrophic areas, and bulk sedimentary $\delta^{15}N$ ($\delta^{15}N_{bulk}$) of core MD12-3433, located in the northern South China Sea (SCS), to explore possible causes of the offset between these two proxies in the SCS. The offset can be best explained by the influence of the terrigenous input on $\delta^{15}N_{bulk}$, as evidenced by its general correlation with sea level changes, C:N ratios, and inorganic nitrogen contribution to total nitrogen. Moreover, our new record is compared to six previously published $\delta^{15}N_{bulk}$ records of the SCS based on their geographical proximity to the mainland or large rivers, which all show being influenced by terrigenous input. The effect of changes in vertical mixing is evaluated and believed to play a minor role on the general pattern of FB-$\delta^{15}N$, while N_2 fixation is the most important impact on FB-$\delta^{15}N$ records in the SCS as previously studies revealed. A deeper mixed layer during the last glacial period could result in nitrate with higher $\delta^{15}N$ from the subsurface being mixed into the euphotic zone. FB-$\delta^{15}N$ of *Orbulina universa* have higher values than *Globigerinoides ruber* and *Globigerinoides sacculifer*, with a maximum difference in the last glacial maximum, which could be accounted for by its deeper habitat where it is sensitive to changes in the contributions of vertically mixed subsurface nitrate relative to nitrate from N_2 fixation.

1. Introduction

Fixed nitrogen (N) is one of the critical limiting nutrients for photosynthesis in vast area of today's ocean. Because of its short residence time (≤3 kyr, [*Codispoti et al.*, 2001]) relative to marine phosphorus (P), its sources and sinks are more sensitive to climate change on the timescale of glacial and interglacial cycles. Hence, the processes that control the sources and sinks of the fixed N inventory can have a significant impact on the strength of the biological pump and thus on atmospheric CO_2 [e.g., *Altabet et al.*, 1995; *Galbraith et al.*, 2008a; *Ganeshram et al.*, 1995]. The primary source of fixed N to the ocean is N_2 fixation by diazotrophic bacteria, with minor inputs from land and atmosphere, and the main sink is denitrification occurring in the sediments and the oxygen minimum zones in the water column [*Galbraith et al.*, 2008a; *Gruber and Galloway*, 2008].

The stable nitrogen isotope ($\delta^{15}N = {}^{15}N/{}^{14}N_{sample} / {}^{15}N/{}^{14}N_{air} - 1$, N_2 in the air is the reference) of organic N provides an important tool for studying the N budget and cycle in the ocean. Due to different kinetic effects of the heavy and light stable isotopes, nitrate uptake by phytoplankton preferentially removes ^{14}N, leaving the residual nitrate pool enriched in ^{15}N. However, no net isotope fractionation would be expressed if nitrate were completely consumed. Therefore, $\delta^{15}N$ of the organic matter produced in oligotrophic regions, where nitrate utilization is complete, should reflect $\delta^{15}N$ of the N source to the euphotic zone, which is mainly from vertical mixing of subsurface nitrate augmented by *in-situ* N_2 fixation, atmospheric N deposition and terrestrial input of organic and inorganic nitrogen. Mean ocean nitrate has a $\delta^{15}N$ value of approximately 5‰ [*Sigman et al.*, 2000]. Since little isotope fractionation occurs during N_2 fixation, the newly

fixed N through N_2 fixation is only slightly lower than that of the air (0 to −2‰, [*Carpenter et al.*, 1997]). Hence, N_2 fixation reduces $\delta^{15}N$ of subsurface nitrate [*Karl et al.*, 2002; *Liu et al.*, 1996] relative to the mean ocean nitrate $\delta^{15}N$. On the other hand, water column denitrification causes a regional increase in the thermocline nitrate $\delta^{15}N$ due to its strong discrimination against ^{15}N [*Altabet et al.*, 1999]. It is generally shown that bulk sedimentary $\delta^{15}N$ ($\delta^{15}N_{bulk}$) records changes in surface ocean $\delta^{15}N$ dynamics. However, the use of $\delta^{15}N_{bulk}$ can be compromised by various processes. First, post-depositional bacterially driven degradation can significantly elevate the ^{15}N of sedimentary N relative to the N sinking out of the surface ocean outside of sedimentary environments characterized by high organic matter preservation (e.g., upwelling areas and continental margins) [*Altabet* and *Francois*, 1994; *Lourey et al.*, 2003]. Second, sedimentary organic N can be contaminated by terrestrial sources of organic and inorganic N, especially in regions near the coasts or with little marine organic matter being preserved and buried [*Kienast et al.*, 2005; *Schubert and Calvert*, 2001].

Ren et al. [2009, 2012b] showed that $\delta^{15}N$ of organic nitrogen bound in foraminifera tests (foraminifera-bound $\delta^{15}N$, or FB-$\delta^{15}N$) can be an effective recorder of thermocline nitrate $\delta^{15}N$ in the oligotrophic areas because FB organic matter is protected from contamination of terrestrial N and organic matter degradation [*Altabet and Curry*, 1989]. Studies using both FB-$\delta^{15}N$ and $\delta^{15}N_{bulk}$ show dramatic differences between the two proxies. In oligotrophic regions with N_2 fixation occurring, including the Caribbean Sea, the Gulf of Mexico and the South China Sea (SCS), FB-$\delta^{15}N$ values are higher in the last ice age relative to the Holocene,

while $\delta^{15}N_{bulk}$ values are not [*Meckler et al.*, 2011; *Ren et al.*, 2009, 2012a]. In these cases, the higher glacial FB-$\delta^{15}N$ values are interpreted to represent reduced N_2 fixation, and the lack of $\delta^{15}N_{bulk}$ change is considered to result from the counteracting effect of greater terrigenous input in the glacial sediment which lowers $\delta^{15}N$ of the total bulk sedimentary N. In addition, the published $\delta^{15}N_{bulk}$ records in the SCS show varying amplitudes of glacial to interglacial changes from nearly no difference to slightly higher Holocene values, but none of them are similar to the FB-$\delta^{15}N$ trends [*Kienast*, 2000; *Higginson et al.*, 2005]. As for the FB-$\delta^{15}N$, species offsets have been observed even within dinoflagellate symbiont-bearing planktonic species [*Ren et al.*, 2009, 2012a]. In a plankton tow study, it appeared that suspended particulate organic matter (POM), as part of N source of deeper-dwelling species, may account for their slightly higher values relative to the surface-dwellers, but much work still remains [*Ren et al.*, 2012b]. Therefore, the causes of both the offset between $\delta^{15}N_{bulk}$ and FB-$\delta^{15}N$ and the species-specific FB-$\delta^{15}N$ offset in downcore records need to be further explored and assessed.

In this study, we analyze FB-$\delta^{15}N$ and $\delta^{15}N_{bulk}$ of core MD12-3433 at the northern SCS over the last 47 ka, and interpret them in comparison with other bulk sediment proxies and the published $\delta^{15}N$ record from MD97-2142 at the southeastern SCS [*Ren et al.*, 2012a] to further analyze the causes of the offset between $\delta^{15}N_{bulk}$ and FB-$\delta^{15}N$, and the offset of FB-$\delta^{15}N$ between of several species.

2. Oceanography Background

The South China Sea is the largest marginal sea in the tropical western North Pacific. The deep water only comes from the adjacent western North Pacific through the Luzon Strait (sill depth ~ 2400 m) between Taiwan and the Luzon Islands [*Qu et al.*, 2006]. In the upper layer (above 500 m), water from the western North Pacific enters the SCS through the Luzon Strait in winter and flows back into the western North Pacific in summer [*Tian et al.*, 2006; *Wyrtki*, 1961]. The surface circulation of the modern SCS has distinct seasonal characteristics driven by the East Asian Monsoon, a large cyclonic gyre in winter and an anti-cyclonic gyre in the south plus a weak cyclonic gyre in the north in summer [*Wyrtki*, 1961; *Liu et al.*, 2002] (Fig. 1). The surface water of the SCS coming from the western North Pacific can be influenced by the Eastern Tropical North Pacific water advected by the North Equatorial Current (Fig. 1). The euphotic layer is oligotrophic and both N and P are usually below the detectable limits [*Chen et al.*, 2004].

Modern observations indicate that the SCS and the surrounding areas are characterized by N_2 fixation. A significant contribution of N_2 fixation to the nutrient inventory was indicated from nitrate anomaly (N*) in the upper thermocline in the northern SCS [*Wong et al.*, 2002]. In addition, thermocline nitrate has relatively low $\delta^{15}N$ values (~4.2‰ [*Wong et al.*, 2002] and ~4.8‰ [*Yang et al.*, 2016]) in the northern SCS, also due to N_2 fixation.

3. Materials and Methods

Core MD12-3433 (19°16.88′N, 116°14.52′E, 2125 m water depth, 8.2 m recovery) was

recovered in 2012 from the northern continental slope of the SCS, approximately 340 km offshore the Pearl River mouth (Fig. 1) during the Chinese-French CIRCEA cruise of R/V Marion Dufresne. The sediment lithology is homogenous and dominated by greenish gray to dark gray clay with several layers abundant with organic matter [*Kissel et al.*, 2012]. The age model is established based on 14 planktonic foraminiferal AMS ^{14}C dates of MD12-3433 (triangles in Fig. 2) through linear interpolation. The average sedimentation accumulation rate is higher during the last glacial (~ 27 cm/ka) than the Holocene (~12 cm/ka).

Three species of euphotic zone-dwelling foraminifera in the >250 μm size fraction, *Globigerinoides ruber*, *Globigerinoides sacculifer* and *Orbulina universa*, were analyzed for FB-δ^{15}N. The protocol for measuring FB-δ^{15}N [*Ren et al.*, 2009; *Ren et al.*, 2012b] includes 1) chemical treatment of the foraminiferal shells to remove external N contamination, followed by acid dissolution of the cleaned shells, 2) conversion of organic nitrogen released into solution to nitrate by persulfate oxidation [*Nydahl*, 1978; *Knapp et al.*, 2005]; 3) measurement of nitrate concentration by chemiluminescence [*Braman* and *Hendrix*, 1989], and (4) bacterial conversion of nitrate to nitrous oxide [*Sigman et al.*, 2001], with measurement of the δ^{15}N of the nitrous oxide by automated extraction and gas chromatography-isotope ratio mass spectrometry [*Casciotti et al.*, 2002]. Specifically, 1 to 5 mg of foraminiferal tests per sample were gently crushed, cleaned first by 5 min ultrasonication in 2% sodium hexametaphosphate (pH 8), then rinsed twice with deionized water (DI). Samples were then treated with persulfate and rinsed five times with DI. The remaining 0.5 to 3 mg of cleaned foraminiferal tests were subsequently

completely dissolved in 6 N hydrochloric acid, releasing organic matter for analysis. Given the small size of materials, no cleaning duplicates were made. We use three organic standards: USGS 40 ($\delta^{15}N$ = -4.5‰), USGS 41 ($\delta^{15}N$ = 47.6‰), and a self-made mixture of 6-aminocaproic acid and glycine ($\delta^{15}N$ = 5.4‰) to correct for the oxidation blanks, which is on average 10% of the sample size. A minimum of 18 organic standards and 3–5 blanks are analyzed per batch of samples. The size of the nitrogen blank relative to sample nitrogen content is ~0.1‰. The $\delta^{15}N$ of the persulfate blank is 4.6‰ as quantified by the organic standards. This is similar to the range of FB-$\delta^{15}N$ measured in our samples. Reproducibility for mass spectrometer analyses is generally better than 0.1‰. FB-$\delta^{15}N$ were analyzed at the Princeton University.

Bulk sediments were sampled every 8 cm (~2 samples/kyr), yielding 103 samples. $\delta^{15}N_{bulk}$ and TN were analyzed on unacidified bulk sediments. A subset of samples were acidified by buffered solution of glacial acetic acid (pH = 5) and repeatedly rinsed with deionized water and centrifuged to remove acid. Carbonate-free samples were then analyzed for $\delta^{13}C_{org}$, TOC and C:N ratios. Sediment samples were run on a Carlo Erba 1108 elemental analyzer, interfaced to a Thermo Finnigan Delta Plus XP IRMS, at the University of California, Santa Cruz.

4. Results

FB-$\delta^{15}N$ of the three species in this study (Fig. 2a) generally have similar range and variability with those in the study of core MD97-2142 [*Ren et al.*, 2012a] (Fig. 2b). The

FB-$\delta^{15}N$ records of the three species all show a glacial-to-interglacial decrease. FB-$\delta^{15}N$ values of both *G. ruber* and *G. sacculifer* started to increase at around 25 ka and show a maximum (~7‰) during the deglaciation at around 15 ka, whereas FB-$\delta^{15}N$ values of *O. universa* show a maximum (~8.5‰) during the LGM at around 24 ka and are generally higher than the other two species, especially during the LGM (Fig. 2a).

Variations in the record of $\delta^{15}N_{bulk}$ are not similar to those in the FB-$\delta^{15}N$ records (Fig 3a and 3b). The range of $\delta^{15}N_{bulk}$ is relatively small, from 4.7‰ to 5.7‰. The record of $\delta^{15}N_{bulk}$ shows no obvious trend from 47 to 19 ka, followed by slightly increasing from 19 ka to reach a maximum at around 7 ka and then slightly decreasing into the late Holocene (Fig. 3b). Other $\delta^{15}N_{bulk}$ records from all over the SCS (Higginson et al., 2003; Kienast, 2000; Ren et al., 2012a) also show little variability during the glacial/interglacial cycles (Fig. 2c).

The range of $\delta^{13}C_{org}$ is from −20.0‰ to −21.7‰, increasing progressively during Marine Isotope Stage (MIS) 3 (average ~ −20.8‰), reaching around −20.5‰ during the LGM and early deglaciation, and then decreasing during the deglaciation to average Holocene value of −21.2‰ (Fig. 3c). The C:N ratios also increased progressively during MIS 3 (the average ~ 6.6), reached a maximum around 8.6 during the LGM and early deglaciation, and then decreased to the late Holocene (the average ~ 7.3) (Fig. 3d). Similar to the records of $\delta^{13}C_{org}$ and C:N ratio, both TOC and TN values were higher during the last glacial period and early deglaciation than the Holocene (Fig. 3e and 3f).

5. Discussion

5.1 $\delta^{15}N_{bulk}$ in the SCS

Variations in the $\delta^{15}N_{bulk}$ record are unrelated to those of the FB-$\delta^{15}N$ records at both MD12-3433 (this study) and eastern SCS core MD97-2142 [*Ren et al.*, 2012a]. Except for the $\delta^{15}N_{bulk}$ record from ODP 1144 in the northern SCS, which shows trends possibly due to sediment drift and allochthonous origin of both organic and inorganic nitrogen [*Higginson et al.*, 2003; *Kienast et al.*, 2005], most published $\delta^{15}N_{bulk}$ records [*Kienast*, 2000] show no clear glacial/interglacial variability, particularly when compared with FB-$\delta^{15}N$ records (Fig. 2c). The lack of obvious glacial/interglacial $\delta^{15}N_{bulk}$ change among these different records was thus used to infer that ocean nitrate $\delta^{15}N$ was constant [*Kienast*, 2000]. However, the fidelity of $\delta^{15}N_{bulk}$ as a proxy of nitrate $\delta^{15}N$ in the SCS was challenged since N contributions from land [*Kienast et al.*, 2005] and alteration during burial [*Robinson et al.*, 2012] can result in misleading $\delta^{15}N_{bulk}$ records. The sharp contrast between FB-$\delta^{15}N$ and $\delta^{15}N_{bulk}$ records reconfirms the infidelity. The effect of terrigenous input and alteration during burial on $\delta^{15}N_{bulk}$ needs further exploration.

$\delta^{13}C_{org}$ and C:N ratios in sediments are widely used to discriminate organic matter of terrestrial and marine origins [e.g., *Knudson et al.*, 2015; *Meckler et al.*, 2011; *Meyers*, 1994]. A SCS study of sediment cores, plankton and particulate organic matter (POM) from the coastal area off-shore the Pearl River estuary demonstrates that $\delta^{13}C_{org}$ and C:N are reliable geochemical indicators of organic matter of marine or terrestrial origin [*Chen et al.*, 2008]. Terrestrial organic material deposited in the northern SCS has a $\delta^{13}C$ value and C:N ratio of

−25.5‰ and 22, respectively, and marine organic matter has values of −22.1‰ and 6.6, respectively [*Liu et al.*, 2007].

During the glacial period, there was higher input of fine-grained terrestrial sediment from the South China due to low sea-level [*Liu et al*., 2016; *Zhang et al.*, 2016]; this observation is consistent with the record of C:N ratios in our study of core MD12-3433 (Fig. 3c), which are relatively high during the glacial, especially in the last deglaciation and the LGM. The peak C:N ratios in the LGM are ~9, which are just above the marine end member and well below pure terrestrial end member value, indicating that while the majority of organic matter is of marine origin throughout our record, there may be significant contributions of N from land. C:N is used to quantify the changes of terrestrial input, showing that the contribution from terrestrial input was higher than 10% during the LGM and lower than 10% during the Holocene. C:N values may also be affected by the addition of inorganic nitrogen, mostly from ammonia derived from organic matter decomposition, absorbed on clays [*Hu et al.*, 2006; *Meyers*,1997]. Therefore, it is just a rough estimate of quantification, which shows higher terrestrial input during the LGM.

Because terrestrial organic matter has relatively low $\delta^{13}C_{org}$ values, it might be expected that our $\delta^{13}C_{org}$ values would be lower during the glacial period to corroborate our interpretation, based on the C:N record, of higher terrestrial input during the glacial. Instead, the $\delta^{13}C_{org}$ record shows relatively high $\delta^{13}C_{org}$ values during the glacial stage. Therefore, it is likely that the $\delta^{13}C_{org}$ signal of changing amounts of terrigenous organic matter was overprinted by other processes related to changes in biological productivity. In core MD12-3433, the $\delta^{13}C_{org}$ values range from

−20.0‰ to −21.7‰, indicating that the organic matter is generally of marine origin, and the records of TOC and TN content (Fig. 3d and 3e) indicate higher productivity during the last glacial, especially in the last deglaciation and the LGM. In addition, the sedimentation rate is relatively high during the glacial period (Fig. 4) also supports that the high TOC and TN content can reasonably be interpreted as indicative of higher productivity. Other proxy records from the northern SCS support the idea that there was higher productivity in the last glacial period, including TOC and chlorine abundance records from ODP Site 1144 [*Higginson et al.*, 2003], an alkenone content record from core SO50-31KL [*Huang et al.*, 1997], and a record of relative abundance of *Florisphaera profunda* (%FP) from cores MD12-3428 [*Zhang et al.*, 2016] and MD05-2904 [*Su et al.*, 2013]. Higher productivity during glacials in the northern SCS is generally attributed to enhanced vertical mixing in response to a strengthened East Asian Winter Monsoon (EAWM) bringing subsurface nutrients into the euphotic zone [*Wang and Li*, 2003]. Phytoplankton discriminate heavy carbon isotope during photosynthesis rendering a surface carbon reservoir with higher $\delta^{13}C$, and the isotope fractionation itself decreases, also rendering higher $\delta^{13}C_{org}$ values, as pCO_2 is drawn down. As such, higher productivity could explain the elevated glacial $\delta^{13}C_{org}$ values. Thus, while the C:N data point to elevated terrigenous inputs during the glacial, the $\delta^{13}C_{org}$ record does not support it. Different proxy records of bulk sediment are confusing. However, further insight into the interpretation of the $\delta^{15}N_{bulk}$ record can be achieved by comparing it to the FB-$\delta^{15}N$ record.

In oligotrophic regions like the SCS, the time-averaged total organic matter produced in

the surface ocean, if well-preserved in the sediment, should have the same $\delta^{15}N$ value as the nitrate source to the euphotic zone, which is mainly from the upper thermocline. FB-$\delta^{15}N$ of the euphotic zone dwelling foraminiferal species closely record thermocline nitrate $\delta^{15}N$. We can thus use the difference between FB-$\delta^{15}N$ (average of three species) and $\delta^{15}N_{bulk}$ measurements to infer sedimentary processes altering $\delta^{15}N_{bulk}$. The $\delta^{15}N_{bulk}$ is lower than FB-$\delta^{15}N$ in the last glacial period, but higher in the Holocene (Fig. 4). A similar pattern is observed at MD97-2142 [*Ren et al.*, 2012a] (Fig. 4). The $\delta^{15}N$ differences in the two cores vary almost synchronously with the sea level changes (Fig. 4). This could be explained by accounting for the fact that more fine-grained sediments reached the deep SCS during low sea level stand [*Liu et al.*, 2016; *Zhang et al.*, 2016]. One possibility is that when sea level was low and the coastline was closer to the shelf break, riverine-derived sediment was delivered more directly to the upper slope and to the core location; in contrast, during high sea level stands, riverine-derived sediment would have been deposited on the shelf prohibiting direct deposition near the shelf break or the core site. Sedimentation rate (Fig. 4) was higher during the LGM and MIS 3, indicating that more riverine-derived sediment deposited in the core location.

In fact, we find a positive correlation at both sites when comparing the difference between FB-$\delta^{15}N$ and $\delta^{15}N_{bulk}$ with C:N ratios, whose R^2 are 0.59 and 0.75 for core MD12-3433 and MD12-2142, respectively (Fig. 5). Since the C:N ratio is an indicator of the relative contributions of terrigenous organic matter, its correlation to the difference between FB-$\delta^{15}N$ and $\delta^{15}N_{bulk}$ could also be explained by changes in the input of terrigenous organic matter if the

$\delta^{15}N$ of the terrigenous end members were relatively low.

The $\delta^{15}N$ of the surface sediments, believed to be of terrigenous origin, from the Pearl River mouth, ranges between 6.2 and 7.1‰ at present [*Gaye et al.*, 2009], 1-2‰ higher than the modern thermocline nitrate [*Wong et al.*, 2002], due to Pearl River pollutants and sedimentary denitrification in the inner shelf which strongly modifies the $\delta^{15}N$ of the sediments [*Gaye et al.*, 2009]. Further evidence that anthropogenic activity, including rapid coastal development, has resulted in enhanced $\delta^{15}N_{bulk}$ values can be found in sediment records spanning the last century from offshore the Pearl River [*Jia et al.*, 2013]. Moreover, denitrification is found occurring over the watershed of the Pearl River indicated by the $\delta^{15}N$ and $\delta^{18}O$ signal [*Chen et al.*, 2009]. On the other hand, the $\delta^{15}N$ of the less polluted rivers discharging into the SCS is similar or slightly lower than the modern thermocline nitrate $\delta^{15}N$. For example, the Mekong River has a $\delta^{15}N$ signal of around 4.2, which seems to be typical of large tropical rivers [*Gaye et al.*, 2009]. We speculate that the Pearl River discharge may have had a similarly low $\delta^{15}N$ signature before it was polluted. Therefore, since it is widely observed in the SCS that terrigenous input was greater in the glacials, it is reasonable to explain the lower glacial $\delta^{15}N_{bulk}$ value relative to FB-$\delta^{15}N$ by greater terrigenous input during the glacials. Furthermore, the general correlation between C:N and the difference between FB-$\delta^{15}N$ and $\delta^{15}N_{bulk}$ (Fig. 5) is best explained by changes in terrigenous input over the last ~40 ka. However, $\delta^{15}N$ of terrestrial end members in the past could have been different from its present values, thus must be interpreted cautiously.

While $\delta^{15}N_{bulk}$ is assumed to primarily reflect the nitrogen isotopic composition of marine

organic fraction, it can also be influenced by the inorganic fraction. Terrestrial inorganic nitrogen (N_{inorg}) usually has a lower $\delta^{15}N$ than marine organic nitrogen [*Kienast et al.*, 2005; *Schubert and Calvert*, 2001]. Therefore, the $\delta^{15}N_{bulk}$ signal can be dampened because of terrestrial inorganic nitrogen input. The TOC versus TN linear relationship shows an intercept of 0.066 (Fig. 6), which was approximated as the contribution of N_{inorg} to TN, implying 38–66% of N_{inorg} contribution to TN. Isotopic analysis of inorganic fraction in sediment traps in the SCS from *Kienast et al.* [2005] reveals that N_{inorg} have $\delta^{15}N$ values ranging from 3.1 to 4.8‰, which accounts for dampening of our $\delta^{15}N_{bulk}$ values ranging from 0.58 to 3.31‰. In conclusion, varying amounts of terrigenous N input, including inorganic N input, influence $\delta^{15}N_{bulk}$ records in the SCS, which may be controlled by the sea level change and its influence on the delivery of riverine-derived sediment to the sites MD12-3433 and MD97-2142.

Although the variability in most $\delta^{15}N_{bulk}$ records from the SCS is weak (Fig. 7) compared with the FB-$\delta^{15}N$ records (Fig. 2) due to overprinting of the $\delta^{15}N_{bulk}$ records by changes in terrigenous input especially during the glacials, they may still hold some meaningful information. The $\delta^{15}N_{bulk}$ values from core 18284 are markedly lower than other records, and MD97-2142 and 17954 (named “the first group” thereafter) are slightly higher than other records (Fig. 7). $\delta^{15}N_{bulk}$ values of MD12-3433, 17940, 17924 and 17961 (named “the second group” thereafter) are between the first group and 18284. 18284 is located close to the Sunda Shelf and during the low sea level stand of the LGM it was in close proximity to the emerging land (Fig. 1). Bulk sedimentary $\delta^{13}C_{org}$ for 18284 were approximately −21% at the core top

suggesting a mostly marine origin of organic matter, whereas $\delta^{13}C_{org}$ values were depressed and reached approximately −26% in the LGM indicating the presence of significant amounts of terrigenous organic matter [*Kienast et al.*, 2005]. Therefore, the $\delta^{15}N_{bulk}$ record of 18284 is influenced strongly by terrigenous input with relative low $\delta^{15}N$ signature. In contrast, $\delta^{13}C_{org}$ for other cores in Fig. 7 all range between −19% and −22% [*Kienast et al.*, 2001; *Ren et al.*, 2012a], close to the end member of marine organic matter. The first group of the two cores is further away from large rivers than the second group consisting of three cores located offshore of the Pearl River and one core (17961) located in the vicinity of the Sunda Shelf offshore of the Mekong River. Thus, the decreasing $\delta^{15}N_{bulk}$ values, from the first group to the second group and then to core 18284, could reflects differences in terrigenous input due to their geographical proximity.

In regions with high sediment accumulation rates and high productivity, little offset is found between $\delta^{15}N_{bulk}$ of surface sediment and that of sinking particles indicating minimal impact of diagenesis on $\delta^{15}N_{bulk}$ in these environments [*Altabet et al.*, 1999; *Kienast et al.*, 2002]. However, in environments with low sediment accumulation, $\delta^{15}N_{bulk}$ could increase due to degradation in the water column and diagenetic alteration, generally due to the preferential loss of ^{14}N during the oxidation of organics [*Galbraith et al.*, 2008a; *Lahajnar et al.*, 2007; *Robinson et al.*, 2012]. Organic matter degradation can be particularly intense in the water column and at the sediment-water interface when water masses are well-ventilated and primary productivity is relatively low [*Lahajnar et al.*, 2007]. Degradation of organic matter in the

surface sediments occurs all over the SCS [*Gaye et al.*, 2009]. Therefore, in addition to the influence of the terrigenous input, degradation of organic matter could influence the offset between FB-$\delta^{15}N$ and $\delta^{15}N_{bulk}$ values, especially during the Holocene when sedimentation rate and productivity were relatively low and the deep ventilation was relatively strong in the SCS [*Wan* and *Jian*, 2014]. Thus, the relatively high $\delta^{15}N_{bulk}$ values, compared to FB-$\delta^{15}N$, in the Holocene in both MD12-3433 and MD97-2142 may be partially influenced by degradation and diagenetic alteration of the bulk organic material. Future work focused on generating proxy records of ventilation, productivity and degradation could help to untangle the effects of these processes on $\delta^{15}N_{bulk}$ records. In conclusion, in coastal environments without high sediment accumulation rates and high productivity, like the SCS, terrigenous input is the primary influence, meanwhile degradation and diagenetic alteration can also impact the $\delta^{15}N_{bulk}$ record and obscure the primary signal related to changes in the $\delta^{15}N$ of POM in the surface water.

5.2 FB-$\delta^{15}N$ of three species in the SCS

The FB-$\delta^{15}N$ records of the three species in this study all show a glacial-to-interglacial decrease (Fig. 2a), similar to the higher resolution record at MD97-2142 at southeastern SCS (Fig. 2b) [*Ren et al.*, 2012]. Since a significant glacial-to-interglacial change in global mean ocean nitrate $\delta^{15}N$ is unlikely [*Brandes* and *Devol*, 2002; *Deutsch et al.*, 2004], lower interglacial FB-$\delta^{15}N$ in our record and in MD97-2142 is most likely caused by an increase of N_2 fixation depressing $\delta^{15}N$ of nitrate regionally. While there is a generally decreasing

glacial-to-interglacial trend in all three species of FB-$\delta^{15}N$ records (Fig 2), they differ in detail during the last deglaciation and the LGM. FB-$\delta^{15}N$ of *G. ruber* and *G. sacculifer* have maximum values in the deglaciation, whereas FB-$\delta^{15}N$ of *O. universa* has maximum values in the LGM. FB-$\delta^{15}N$ maxima of *G. ruber* and *G. sacculifer* in the deglaciation are most likely reflecting the influence of open ocean nitrate $\delta^{15}N$, as observed in core MD97-2142. Nitrate $\delta^{15}N$ was relatively high during the deglaciation as observed in records both within major water column denitrification zones [e.g., *Altabet et al.*, 2002; *Ganeshram et al.*, 1995; *Hendy* and *Pedersen*, 2006; *Higgison* and *Altabet*, 2004] and outside these zones, such as in the east equatorial Pacific [*Robinson et al.*, 2009], eastern North Pacific [*Hendy et al.*, 2004; *Emmer* and *Thunell*, 2000; *Kienast et al.*, 2002], eastern subarctic Pacific [*Galbraith et al.*, 2008b], northern Chile [*De Pol-Holz et al.*, 2006], Caribbean Sea [*Ren et al.*, 2009], western North Pacific [*Jia et al.*, 2011; *Kao et al.*, 2008] and SCS [*Ren et al.*, 2012a]. Although the deglaciation $\delta^{15}N$ maximum signal in some areas may be overprinted by other changes in the nitrate $\delta^{15}N$ of source water, N_2 fixation and/or nitrate utilization, the dominance of the $\delta^{15}N$ maximum in records throughout the western North and tropical Pacific [*Jia et al.*, 2011; *Kao et al.*, 2008] suggests that the signal of intensified water column denitrification during the deglaciation was transported to areas outside of major denitrification zones, and specifically into the SCS.

While the main FB-$\delta^{15}N$ pattern in this study can be explained by changes in the $\delta^{15}N$ of the source water and N fixation as described above, the possible effect of changes in vertical mixing also needs to be evaluated. Measurement of nitrate $\delta^{15}N$ in the northern SCS [*Wong et*

al., 2002; *Yang et al.*, 2016] indicates that $\delta^{15}N$ increases by about 1‰ from 100 m to 300 m. Thus, theoretically, deeper mixing could result in a slight increase in the $\delta^{15}N$ of source water; but, our FB-$\delta^{15}N$ record includes changes greater than 1‰, and thus the primary signal cannot be explained by changes in vertical mixing alone. Here we explore whether changes in vertical mixing may explain some of the low amplitude secondary fluctuations in our records by examining changes in the thermal gradient between surface and thermocline waters (Fig. 8). These upper water thermal gradients (ΔT), the difference between the sea surface temperature (SST) and the thermocline water temperature (TWT) derived from Mg/Ca of *G. ruber* and of *Pulleniatina obliquiloculata*, respectively, were from core MD12-3432, located at the same location as MD12-3433, MD12-3434 and MD05-2904 [*Steinke et al.*, 2011], both located close to MD12-3433 in the northern SCS (Fig. 1). *P. obliquiloculata* is a thermocline-dwelling planktic foraminiferal species living within 100-150 m in tropics [*Dang et al.*, 2012; *Xu et al.*, 2006]. To reconcile these records, SST and TWT derived from Mg/Ca from MD05-2904 [*Steinke et al.*, 2011] were recalculated using the equations from *Huang et al.*, (2008) and *Anand et al.* (2003), respectively, so that they could be directly compared with the data from MD12-3432 and MD12-3434. ΔT can reflect the depth of thermocline (DOT) [e.g., *Steinke et al.*, 2010], with higher values indicating shallower DOT and less vertical mixing, and vice versa.

The ΔT patterns (Fig. 8) represent that the depth of thermocline (DOT) was deeper during the LGM compared with the Holocene, which was most likely driven by stronger East Asian Winter Monsoon (EAWM). Deeper mixing during the glacials is also observed at other locations

in the SCS [*Li et al.*, 2013; *Steinke et al.*, 2010; *Tian et al.*, 2005]. The two data points of MD12-3433 that indicate deeper mixing during the deglaciation are not corroborated by the other two higher resolution records (Fig. 8c); as such, our discussion is focused on the more robust observation of deeper mixing during the LGM compared with the Holocene. It is noted that when the DOT and vertical mixing were relatively deep and strong during the LGM, the FB-δ^{15}N values of *G. ruber* and *G. sacculifer* in this study and all three species of MD97-2142 [*Ren et al.*, 2012] were generally higher, and the DOT became deeper earlier than 20 ka as FB-δ^{15}N values became larger. Therefore, it is suggested that stronger diapycnal mixing during the last glacial time could have brought nitrate with higher δ^{15}N from deeper water [*Wong et al.*, 2002; *Yang et al.*, 2016] to the euphotic zone. In a study in the modern northern SCS, the annual cycle of particulate nitrogen δ^{15}N collected in the upper 200 m resembled that of the mixing layer depth variation with the highest δ^{15}N values during periods of the deepest mixing layer depth, indicating that the seasonal pattern of particulate isotopic composition might be associated with nutrient supply via diapycnal mixing [*Kao et al.*, 2012]. Using the seasonal effect of diapycnal mixing on upper layer δ^{15}N as an analog, the relatively high FB-δ^{15}N values of the LGM may be partially explained by stronger mixing at that time. As mentioned above, this mechanism alone can only explain variations of about 1‰, and thus, as explained earlier, changes in δ^{15}N values of the source due to denitrification and regional changes in N fixation, must be the primary explanation for our FB-δ^{15}N records in the SCS.

The values of FB-δ^{15}N of *O. universa* are higher than those of the other two species,

especially during the LGM (Fig. 2a). Species differences were also observed in MD97-2142 [*Ren et al.*, 2012] and Caribbean Sea [*Ren et al.*, 2009] with the maximal species difference also occurring at the LGM. These differences can be explained by differences in depth habitat of these species. In the modern SCS, both *G. ruber* and *G. sacculifer* inhabit the upper 50 m, *O. universa* grows deeper at ~ 80 m [*Luo et al.*, 2015], and N_2 fixation occurs mainly in the upper 60 m in the modern northern SCS [*Chen et al.*, 2004]. Thus, while the relatively high FB-$\delta^{15}N$ values in all species can generally be attributed to reduced N-fixation during the LGM compared to the Holocene, the larger species offset at the LGM (Fig. 8) could be explained by differences in the relative effect of N_2 fixation and subsurface supply on different depths of the euphotic zone inhabited by different foramininferal species. In particular, the relatively deep habitat of *O. universa*, near the bottom of the mixed layer, makes this species more sensitive to variations in vertical mixing of the subsurface nitrate supply. Stronger vertical mixing (Fig. 8c) during the LGM could therefore explain the enhanced offset between *O. universa* and the other two species (Fig. 8a and 8b).

Planktonic foraminifera obtain part of their N from particulate organic matter (POM), thus POM $\delta^{15}N$ would influence FB-$\delta^{15}N$. From the modern study in the northern SCS, POM $\delta^{15}N$ in the upper 100 m is mostly uniform, whereas POM $\delta^{15}N$ in the 100-200m is consistently higher [*Kao et al.*, 2012]. This downward increasing trend in POM $\delta^{15}N$ may be accounted for by the isotope fraction during remineralization, since light nitrogen would be preferentially recycled during remineralization. In addition, POM $\delta^{15}N$ values from the upper 200 m vary seasonally,

with the highest $\delta^{15}N$ values during periods with the deepest mixing layer depth [*Kao et al.*, 2012]. Moreover, from the plankton tow samples in the Sargasso Sea, *O. universa*, compared to *G. ruber* and *G. sacculifer* and other asymbiotic species, shows greatest variation and strongest correlation with changes in the sinking POM $\delta^{15}N$ [*Ren et al.*, 2012b]. Since POM $\delta^{15}N$ in the 100-200 m is consistently higher than that in the 0-100 m in the SCS [*Kao et al.*, 2012], it is believed that FB-$\delta^{15}N$ of *O. universa* can be more sensitive to the changes in the sinking POM $\delta^{15}N$ due to its deeper habitat. During glacials, higher productivity in the SCS could increase $\delta^{15}N$ of POM thereby additionally causing the larger offset between species at that time.

FB-$\delta^{15}N$ of the three species from southeastern site MD97-2142 [*Ren et al.*, 2012] are generally similar to our data at northern site MD12-3433, but in detail there are differences in how the species offsets change with time. This may be due to geographical differences in the effect of the East Asian Monsoon (wind forcing) on the N_2 fixation depth and/or a different thermocline depth. More detailed oceanographic studies that compare the northern and the eastern SCS are needed to explain our results more completely.

6. Summary

Here we report the differences between FB-$\delta^{15}N$ and $\delta^{15}N_{bulk}$ of core MD12-3433, located in the northern SCS, which is believed to be mostly influenced by terrigenous input, evidenced by its general correlation with sea level changes, C:N ratios, and inorganic nitrogen (N_{inorg}) contribution to total nitrogen. Six more previously published $\delta^{15}N_{bulk}$ records of the SCS in

addition to the record in this study are compared based on their geographical proximity to the mainland or large rivers and present being influenced by terrigenous input. In conclusion, terrigenous input can strongly obscure how the real $\delta^{15}N$ signal of the surface water is recorded in $\delta^{15}N_{bulk}$ all over the SCS. Degradation and diagenetic alteration of organic matter can also play a role on the offset of $\delta^{15}N_{bulk}$.

The effect of changes in vertical mixing is evaluated and believed to play a role on the general pattern of FB-$\delta^{15}N$, although N_2 fixation has the most important effect on FB-$\delta^{15}N$ records in the SCS. A deeper mixed layer during the last glacial period could result in more nitrate with higher $\delta^{15}N$ from the subsurface being mixed into the euphotic zone. FB-$\delta^{15}N$ of *O. universa* have higher values than *G. ruber* and *G. sacculifer*, with a maximum in the LGM, which could be accounted for by its deeper habitat depth that renders it more sensitive to the relative contributions of nitrate from the upward mixing of subsurface and from N_2 fixation. During the glacials, FB-$\delta^{15}N$ of *O. universa* could have been further enhanced by due to the uptake of POM with higher $\delta^{15}N$ from deeper layer and higher productivity.

This study emphasizes the influence of terrigenous input on the $\delta^{15}N_{bulk}$ and reconfirms the infidelity of $\delta^{15}N_{bulk}$ as a recorder of sinking organic matter $\delta^{15}N$ in the SCS, and possibly other similar environments. Future work should be aimed at evaluating the causes of the differences between different foraminiferal species to improve FB-$\delta^{15}N$ as a confident recorder for surface ocean $\delta^{15}N$ dynamics.

Acknowledgements. This work was funded by National Natural Science Foundation of China (No. 91428310, 41630965 and 41376045) and the State Oceanic Administration of China (No. GASI-GEOGE-04) (to Z. J. and H. J.), and also funded by NSF Grant OCE-1405178 (to A.C.R.). The complete dataset of this study are available on pangaea.de and mlab.tongji.edu.cn, or upon request from jian@tongji.edu.cn. We would like to thank the France-China joint organization LIA-MONOCL for providing the materials of core MD12-3433. We also thank Dyke Andreasen, Colin Carney, Wilson Sauthoff, Michelle Kim Drake and Sarah White for laboratory assistance, and Yue Wang for his helpful discussion. The constructive comments given by the anonymous reviewers are also appreciated.

References

Altabet, M. A. and W. B. Curry (1989), Testing models of past ocean chemistry using foraminifera $^{15}N/^{14}N$, *Global Biogeochem. Cycles*, *3*(2), 107-119, doi: 10.1029/GB003i002p00107.

Altabet, M. A. and R. Francois (1994), Sedimentary nitrogen isotopic ratio as a recorder for surface ocean nitrate utilization, *Global Biogeochem. Cycles*, *8*(1), 103-116, doi: 10.1029/93GB03396.

Altabet, M. A., R. Francois, D. W. Murray, and W. L. Prell (1995), Climate-related variations in denitrification in the Arabian Sea from sediment $^{15}N/^{14}N$ ratios, *Nature*, *373*(6514), 506-509, doi:10.1038/373506a0.

Altabet, M. A., C. Pilskaln, R. Thunell, C. Pride, D. Sigman, F. Chavez, and R. Francois (1999), The nitrogen isotope biogeochemistry of sinking particles from the margin of the eastern North Pacific, *Deep Sea Res., Part I*, *46*, 655–679, doi:10.1016/S0967-0637(98)00084-3.

Altabet, M. A., M. J. Higginson, and D. W. Murray (2002), The effect of millennial-scale changes in Arabian Sea denitrification on atmospheric CO_2, *Nature*, *415*(6868), 159–162, doi:10.1038/415159a.

Anand, P., H. Elderfield, and M. H. Conte (2003), Calibration of Mg/Ca thermometry in planktonic foraminifera from sediment trap time series, *Paleoceanography*, *18*(2), 1050, doi:10.1029/2002PA000846.

Braman, R. S., and S. A. Hendrix (1989), Nanogram nitrite and nitrate determination in environmental and biological materials by V(III) reduction with chemiluminescence detection, *Anal. Chem.*, *61*, 2715–2718, doi:10.1021/ac00199a007.

Brandes, J. A., and A. H. Devol (2002), A global marine-fixed nitrogen isotopic budget: Implications for Holocene nitrogen cycling, *Global Biogeochem. Cycles*, *16*(4), 1120, doi:10.1029/2001GB001856.

Carpenter, E. J., H. R. Harvey, B. Fry, and D. G. Capone (1997), Biogeochemical tracers of the marine cyanobacterium Trichodesmium, *Deep Sea Res. Part I: Oceanographic Research Papers*, *44*(1), 27-38.

Casciotti, K. L., D. M. Sigman, M. G. Hastings, J. K. Bohlke, and A. Hilkert (2002), Measurement of the oxygen isotopic composition of nitrate in seawater and freshwater using the denitrifier method, *Anal. Chem.*, *74*(19), 4905–4912, doi:10.1021/ac020113w.

Chen, Y.-l. L., H.-Y. Chen, D. M. Karl, and M. Takahashi (2004), Nitrogen modulates phytoplankton growth in spring in the South China Sea, *Cont. Shelf Res.*, *24*(4), 527-541, doi:10.1016/j.csr.2003.12.006.

Chen, F., L. Zhang, Y. Yang, and D. Zhang (2008), Chemical and isotopic alteration of organic matter during early diagenesis: Evidence from the coastal area off-shore the Pearl River estuary, south China, *Journal of Marine Systems*, *74*(1): 372-380, doi:10.1016/j.jmarsys.2008.02.004.

Chen, F., G. Jia and J. Chen (2009), Nitrate sources and watershed denitrification inferred from nitrate dual isotopes in the Beijiang River, south China, *Biogeochemistry*, *94*, 163–174, doi:10.1007/s10533-009-9316-x.

Christensen, J. P. (1994), Carbon export from continental shelves, denitrification and atmospheric carbon dioxide, *Cont. Shelf Res.*, *14*, 547–576,

doi:10.1016/0278-4343(94)90103-1.

Codispoti, L., J. A. Brandes, J. Christensen, A. Devol, S. Naqvi, H. W. Paerl, and T. Yoshinari (2001), The oceanic fixed nitrogen and nitrous oxide budgets: Moving targets as we enter the anthropocene?, *Scientia Marina*, *65*(S2), 85-105, doi:10.3989/scimar.2001.65s285.

Dang, H., Z. Jian, F. Bassinot, P. Qiao, and X. Cheng (2012), Decoupled Holocene variability in surface and thermocline water temperatures of the Indo-Pacific Warm Pool, *Geophys. Res. Lett.*, *39*, doi: 10.1029/2011GL050154.

De Pol-Holz, R., O. Ulloa, L. Dezileau, J. Kaiser, F. Lamy, and D. Hebbeln (2006), Melting of the Patagonian Ice Sheet and deglacial perturbations of the nitrogen cycle in the eastern South Pacific, *Geophys. Res. Lett.*, *33*, L04704, doi:10.1029/2005GL024477.

Deutsch, C., J. L. Sarmiento, D. M. Sigman, N. Gruber, and J. P. Dunne (2007), Spatial coupling of nitrogen inputs and losses in the ocean, *Nature*, *445*(7124), 163–167, doi:10.1038/nature05392.

Devol, A. H. (2015), Denitrification, anammox, and N_2 production in marine sediments, *Annual review of marine science*, *7*, 403-423, doi:10.1146/annurev-marine-010213-135040.

Emmer, E., and R. C. Thunell (2000), Nitrogen isotope variations in Santa Barbara Basin sediments: Implications for denitrification in the eastern tropical North Pacific during the last 50,000 years, *Paleoceanography*, *15*(4), 377–387, doi:10.1029/1999PA000417.

Galbraith, E. D., D. M. Sigman, R. S. Robinson, and T. F. Pedersen (2008a), Nitrogen in past marine environments, *Nitrogen in the marine environment*, *2*, 1497-1535, doi:10.1016/B978-0-12-372522-6.00034-7.

Galbraith, E. D., M. Kienast, S. L. Jaccard, T. F. Pedersen, B. G. Brunelle, D. M. Sigman, and T. Kiefer (2008b), Consistent relationship between global climate and surface nitrate utilization in the western subarctic Pacific throughout the last 500 ka, *Paleoceanography*, *23*, PA2212, doi:10.1029/2007PA001518.

Ganeshram, R. S., T. F. Pedersen, S. E. Calvert, and J. W. Murray (1995), Large changes in oceanic nutrient inventories from glacial to interglacial periods, *Nature*, *376*(6543), 755-758, doi:10.1038/376755a0 .

Gaye, B., M. Wiesner, and N. Lahajnar (2009), Nitrogen sources in the South China Sea, as

discerned from stable nitrogen isotopic ratios in rivers, sinking particles, and sediments, *Mar. Chem.*, *114*(3), 72-85, doi:10.1016/j.marchem.2009.04.003.

Gruber, N. (2004), The marine nitrogen cycle and atmospheric CO_2, in *Carbon-Climate Interactions*, edited by M. Follows and T. Oguz, pp. 97–148, John Wiley, New York.

Gruber, N., and J. N. Galloway (2008), An Earth-system perspective of the global nitrogen cycle, *Nature*, *451*(7176), 293–296, doi:10.1038/nature06592.

Hendy, I. L., T. F. Pedersen, J. P. Kennett, and R. Tada (2004), Intermittent existence of a southern Californian upwelling cell during submillennial climate change of the last 60 kyr, *Paleoceanography*, *19*, PA3007, doi:10.1029/2003PA000965.

Hendy, I. L., and T. F. Pedersen (2006), Oxygen minimum zone expansion in the eastern tropical North Pacific during deglaciation, *Geophys. Res. Lett.*, *33*, L20602, doi:10.1029/2006GL025975.

Higginson, M. J., J. R. Maxwell, and M. A. Altabet (2003), Nitrogen isotope and chlorin paleoproductivity records from the Northern South China Sea: Remote vs. local forcing of millennial- and orbital-scale variability, *Mar. Geol.*, *201*, 223–250, doi:10.1016/S0025-3227(03)00218-4.

Higginson, M. J., and M. A. Altabet (2004), Initial test of the silicic acid leakage hypothesis using sedimentary biomarkers, *Geophys. Res. Lett.*, *31*(18), doi: 10.1029/2004GL020511.

Hu, J., P. Peng, G. Jia, B. Mai and G. Zhang (2006), Distribution and sources of organic carbon, nitrogen and their isotopes in sediments of the subtropical Pearl River estuary and adjacent shelf, Southern China, *Mar. Chem.*, *98*(2–4), 274–285, doi:10.1016/j.marchem.2005.03.008

Huang, C. Y., P. M. Liew, M. Zhao, T. C. Chang, C. M. Kuo, M. T. Chen, C. H. Wang and L. F. Zhang (1997), Deep sea and lake records of the Southeast Asian paleomonsoons for the last 25 thousands years, *Earth Planet. Sci. Lett.*, *146*, 59–72, doi:10.1016/S0012-821X(96)00203-8.

Huang, K.-F., C.-F. You, H.-L. Lin, and Y.-T. Shieh (2008), In situ calibration of Mg/Ca ratio in planktonic foraminiferal shell using time series sediment trap: A case study of intense dissolution artifact in the South China Sea, *Geochem. Geophys. Geosyst.*, *9*, Q04016, doi:10.1029/2007GC001660.

Jia, G., and Z. Li (2011), Easterly denitrification signal and nitrogen fixation feedback documented in the western Pacific sediments, *Geophys. Res. Lett.*, *38*(24), doi:10.1029/2011GL050021.

Jia, G., S. Xua, W. Chen, F. Lei, Y. Bai, C. Huh (2013), 100-year ecosystem history elucidated from inner shelf sediments off the Pearl River estuary, China, *Mar. Chem.*, *151*(20), 47–55, doi:10.1016/j.marchem.2013.02.005.

Kao, S.-J., K.-K. Liu, S.-C. Hsu, Y.-P. Chang, and M. H. Dai (2008), North Pacific-wide spreading of isotopically heavy nitrogen during the last deglaciation: Evidence from the western Pacific, *Biogeosciences*, *5*(6), 1641–1650, doi:10.5194/bg-5-1641-2008.

Kao, S.-J., J.-Y. Terence Yang, K.-K. Liu, M. Dai, W.-C. Chou, H.-L. Lin, and H. Ren (2012), Isotope constraints on particulate nitrogen source and dynamics in the upper water column of the oligotrophic South China Sea, *Global Biogeochem. Cycles*, 26, GB2033, doi:10.1029/2011GB004091.

Karl, D., A. Michaels, B. Bergman, D. Capone, E. Carpenter, R. Letelier, F. Lipschultz, H. Paerl, D. Sigman, and L. Stal (2002), Dinitrogen fixation in the world's oceans, *Biogeochemistry*, *57*, 47–98, doi:10.1023/A:1015798105851.

Kienast, M. (2000), Unchanged nitrogen isotopic composition of organic matter in the South China Sea during the last climatic cycle: Global implications, *Paleoceanography*, *15*(2), 244–253, doi:10.1029/1999PA000407.

Kienast, M., S. E. Calvert, C. Pelejero, and J. O. Grimalt (2001), A critical review of marine sedimentary $\delta^{13}C_{org}$-pCO_2 estimates: New palaeorecords from the South China Sea and a revisit of other low-latitude δ^{13}Corg-pCO_2 records, *Global Biogeochem. Cycles*, *15*(1), 113-127, doi: 10.1029/2000GB001285.

Kienast, S. S., S. E. Calvert, and T. F. Pedersen (2002), Nitrogen isotope and productivity variations along the northeast Pacific margin over the last 120 kyr: Surface and subsurface paleoceanography, *Paleoceanography*, *17*(4), doi: 10.1029/2001PA000650.

Kienast, M., M. J. Higginson, G. Mollenhauer, T. I. Eglinton, M.-T. Chen, and S. E. Calvert (2005), On the sedimentological origin of down-core variations of bulk sedimentary nitrogen isotope ratios, *Paleoceanography*, *20*, PA2009, doi:10.1029/2004PA001081.

Kissel, C., Z. Jian, and H. Leau (2012), MD190-CIRCEA cruise report, *Ref. OCE/2012/01*, Institut Polaire Francais - Paul Emile Victor (IPEV), Brest.

Knapp, A. N., D. M. Sigman, and F. Lipschultz (2005), N isotopic composition of dissolved organic nitrogen and nitrate at the Bermuda Atlantic time-series study site, *Global Biogeochem. Cycles*, *19*, GB1018, doi:10.1029/2004GB002320.

Knudson, K. P., and A. C. Ravelo (2015), Enhanced subarctic Pacific stratification and nutrient utilization during glacials over the last 1.2 Myr, *Geophys. Res. Lett.*, *42*, doi:10.1002/2015GL066317.

Lahajnar, N., M. G. Wiesner and B. Gaye (2007), Fluxes of amino acids and hexosamines to the deep South China Sea, *Deep-Sea Research I, 54*, 2122–2140, doi:10.1016/j. dsr.2007.08.009.

Li, D.W., M.X. Zhao, J. Tian, L. Li (2013). Comparison and implication of TEX86 and U37 temperature records over the last 356 ka of ODP Site 1147 from the northern South China Sea. *Palaeogeography, Palaeoclimatology, Palaeoecology*, 376, 213–223, doi:10.1016/j.palaeo.2013.02.031.

Liu, K. K., M. J. Su, C. R. Hsueh, and G. C. Gong (1996), The nitrogen isotopic composition of nitrate in the Kuroshio Water northeast of Taiwan: Evidence for nitrogen fixation as a source of isotopically light nitrate, *Mar. Chem.*, *54*, 273–292, doi:10.1016/0304-4203(96)00034-5.

Liu, K.-K., S.-Y. Chao, P.-T. Shaw, G.-C. Gong, C.-C. Chen, and T. Y. Tang (2002), Monsoon-forced chlorophyll distribution and primary production in the South China Sea: Observations and a numerical study, *Deep Sea Res., Part I, 49*, 1387–1412, doi:10.1016/S0967-0637(02)00035-3.

Liu, K.-K., S.-J. Kao, H.-C. Hu, W.-C. Chou, G.-W. Hung, and C.-M. Tseng (2007), Carbon isotopic composition of suspended and sinking particulate organic matter in the northern South China Sea—from production to deposition, *Deep Sea Res. Part II: Topical Studies in Oceanography*, *54*(14), 1504-1527, doi:10.1016/j.dsr2.2007.05.010.

Liu, Z., et al. (2016), Source-to-sink transport processes of fluvial sediments in the South China Sea, *Earth Sci. Rev.*, *153*, 238–273, doi:10.1016/j.earscirev.2015.08.005.

Lourey, M. J., T. W. Trull and D. M. Sigman (2003), Sensitivity of $\delta^{15}N$ of nitrate, surface

suspended and deep sinking particulate nitrogen to seasonal nitrate depletion in the Southern Ocean, *Global Biogeochem. Cycles*, *17*(3), doi: 10.1029/2002GB001973.

Meckler, A. N., H. Ren, D. M. Sigman, N. Gruber, B. Plessen, C. J. Schubert, and G. H. Haug (2011), Deglacial nitrogen isotope changes in the Gulf of Mexico: Evidence from bulk sedimentary and foraminifer-bound nitrogen in Orca Basin sediments, *Paleoceanography*, 26, PA4216, doi:10.1029/2011PA002156.

Meyers, P. A. (1994), Preservation of elemental and isotopic source identification of sedimentary organic matter, *Chemical Geology*, *114*(3–4), 289–302, doi:10.1016/0009-2541(94)90059-0.

Meyers, P. A. (1997), Organic geochemical proxies of paleoceanographic, paleolimnologic, and paleoclimatic processes, *Org. Geochem.*, 27(5–6), 213–250, doi:10.1016/S0146-6380(97)00049-1.

Nydahl, F. (1978), Peroxodisulfate oxidation of total nitrogen in waters to nitrate, *Water Res.*, *12*, 1123–1130, doi:10.1016/0043-1354(78)90060-X.

Qu, T., J. B. Girton, and J. A. Whitehead (2006), Deepwater overflow through Luzon strait, *J. Geophys. Res.: Oceans (1978–2012)*, *111*(C1), doi: 10.1029/2005JC003139.

Ren, H., D. M. Sigman, A. N. Meckler, B. Plessen, R. S. Robinson, Y. Rosenthal, and G. H. Haug (2009), Foraminiferal isotope evidence of reduced nitrogen fixation in the ice age Atlantic Ocean, *Science*, *323*(5911), 244–248, doi:10.1126/science.1165787.

Ren, H., D. M. Sigman, M.-T. Chen, and S.-J. Kao (2012a), Elevated foraminifera-bound nitrogen isotopic composition during the last ice age in the South China Sea and its global and regional implications, *Global Biogeochem. Cycles*, *26*, GB1031, doi:10.1029/2010GB004020.

Ren, H., D. M. Sigman, R. C. Thunell, and M. G. Prokopenko (2012b), Nitrogen isotopic composition of planktonic foraminifera from the modern ocean and recent sediments, *Limnol. Oceanogr.*, *57*(4), 1011–1024, doi:10.4319/lo.2012.57.4.1011.

Robinson, R. S., P. Martinez, L. D. Pena, and I. Cacho (2009), Nitrogen isotopic evidence for deglacial changes in nutrient supply in the eastern equatorial Pacific, *Paleoceanography*, *24*, PA4213, doi:10.1029/2008PA001702.

Robinson, R. S., M. Kienast, A. Luiza Albuquerque, M. Altabet, S. Contreras, R. De Pol Holz,

N. Dubois, R. Francois, E. Galbraith, and T. C. Hsu (2012), A review of nitrogen isotopic alteration in marine sediments, *Paleoceanography*, *27*(4), doi:10.1029/2012PA002321.

Schubert, C. J., and S. E. Calvert (2001), Nitrogen and carbon isotopic composition of marine and terrestrial organic matter in Arctic Ocean sediments: Implications for nutrient utilization and organic matter com- position, Deep Sea Res., Part I, *48*(3), 789–810, doi:10.1016/S0967-0637(00)00069-8.

Sigman, D. M., M. A. Altabet, D. C. McCorkle, R. Francois, and G. Fisher (2000), The $\delta^{15}N$ of nitrate in the Southern Ocean: Nitrogen cycling and circulation in the ocean interior, *J. Geophys. Res.*, *105*(C8), 19,599–19,614, doi:10.1029/2000JC000265.

Sigman, D. M., K. L. Casciotti, M. Andreani, C. Barford, M. Galanter, and J. K. Bohlke (2001), A bacterial method for the nitrogen isotopic analysis of nitrate in seawater and freshwater, *Anal. Chem.*, *73*(17), 4145–4153, doi:10.1021/ac010088e.

Steinke, S., M. Mohtadi, J. Groeneveld, L.-C. Lin, L. Löwemark, M.-T. Chen, and R. Rendle-Bühring (2010), Reconstructing the southern South China Sea upper water column structure since the Last Glacial Maximum: implications for the East Asian winter monsoon development. *Paleoceanography*, *25*, PA2219, doi:10.1029/2009PA001850.

Steinke, S., C. Glatz, M. Mohtadi, J. Groeneveld, Q. Li, and Z. Jian (2011), Past dynamics of the East Asian monsoon: No inverse behaviour between the summer and winter monsoon during the Holocene, *Global Planet. Change*, *78*(3–4), 170–177, doi: 10.1016/j.gloplacha.2011.06.006.

Su, X., C. Liu, L. Beaufort, J. Tian, and E. Huang (2013), Late Quaternary coccolith records in the South China Sea and East Asian monsoon dynamics, *Global Planet. Change*, *111*, 88–96, doi:10.1016/j.gloplacha.2013.08.016.

Tian, J., P. Wang, R. Chen, X. Cheng (2005), Quaternary upper ocean thermal gradient variations in the South China Sea: implications for East Asian monsoon climate. *Paleoceanography*, 20, PA4007, doi: 10.1029/2004PA001115.

Tian, J., Q. Yang, X. Liang, L. Xie, D. Hu, F. Wang, and T. Qu (2006), Observation of Luzon Strait transport, *Geophys. Res. Lett.*, *33*(19), doi: 10.1029/2006GL026272.

Wan, S. and Z. Jian (2014), Deepwater exchanges between the South China Sea and the Pacific since the last glacial period, *Paleoceanography*, *29*(12), 1162-1178, doi:

10.1002/2013PA002578.

Wang, R. and J. Li (2003). Quaternary high-resolution opal record and its paleoproductivity implication at ODP Site 1143, southern South China Sea, *Chin. Sci. Bull.*, *48*, 363–367, doi: 10.1007/BF03183231.

Wong, G. T. F., S.-W. Chung, F.-K. Shiah, C.-C. Chen, L.-S. Wen, and K.-K. Liu (2002), Nitrate anomaly in the upper nutricline in the northern South China Sea—Evidence for nitrogen fixation, *Geophys. Res. Lett.*, *29*(23), 2097, doi:10.1029/2002GL015796.

Wyrtki, K. (1961), Physical oceanography of the Southeast Asian waters, NAGA report, Scripps Inst. of Oceanogr.Univ. of Calif, La Jolla.

Xu, J., W. Kuhnt, A. Holbourn, N. Andersen, and G. Bartoli (2006), Changes in the vertical profile of the Indonesian Throughflow during Termination II: Evidence from the Timor Sea, *Paleoceanography*, *21*, PA4202, doi:10.1029/2006PA001278.

Yang, J.-Y. T., S.-J. Kao, M. Dai, X. Yan, and H.-L. Lin (2017), Examining N cycling in the northern South China Sea from N isotopic signals in nitrate and particulate phases, *J. Geophys. Res. Biogeosci.*, *122*, 2118–2136, doi:10.1002/2016JG003618.

Zhang, H., C. Liu, X. Jin, J. Shi, S. Zhao, and Z. Jian (2016), Dynamics of primary productivity in the northern South China Sea over the past 24,000 years, *Geochem. Geophys. Geosyst.*, *17*, 4878–4891, doi:10.1002/ 2016GC006602.

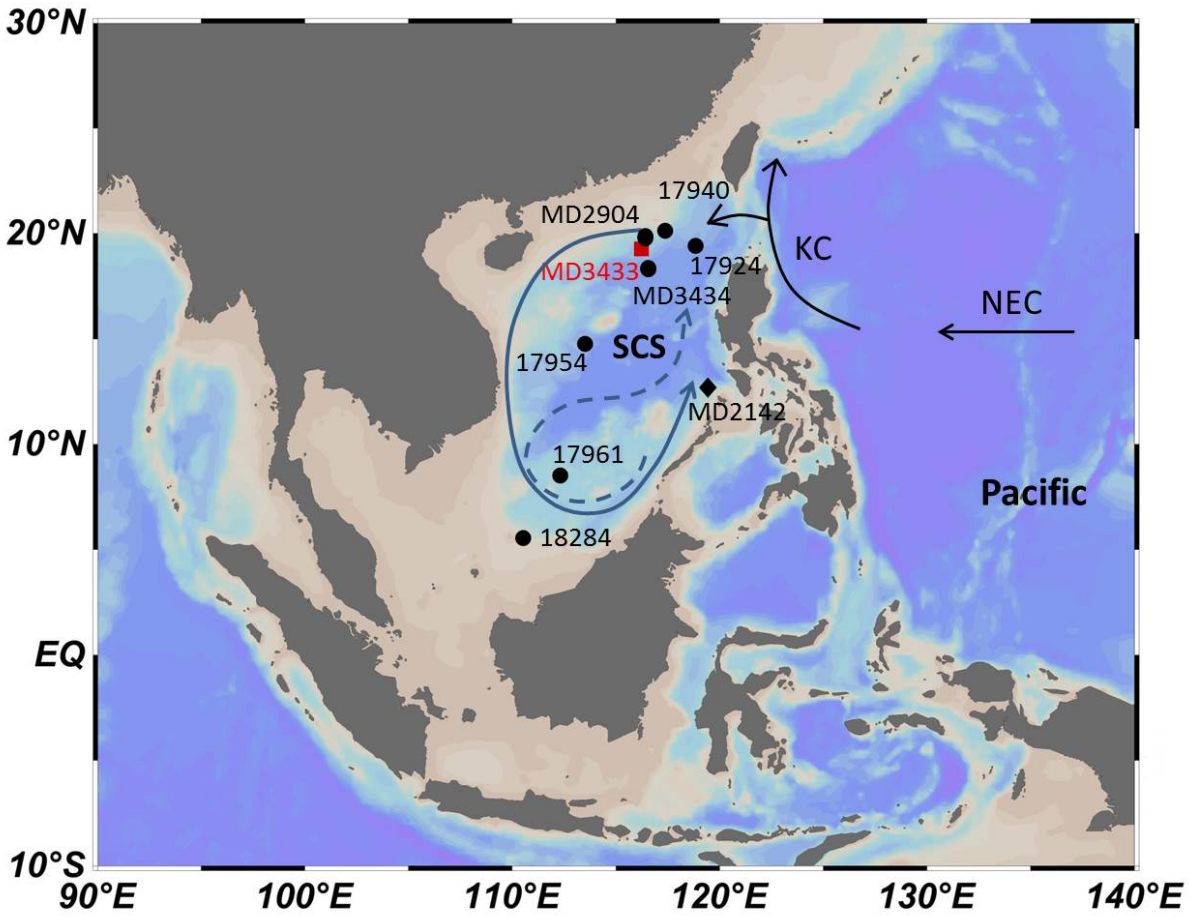

Figure 1. Location map of the SCS and sediment cores. The red square is core MD12-3433 in this study. The black diamond is core MD97-2142 (Ren et al., 2012a). The solid and the dashed curves with arrows within the SCS indicate the general surface circulation in winter and summer, respectively. Also shown are the North Equatorial Current (NEC) and Kuroshio Current (KC), presented by arrows. Khaki areas are emerging lands during the LGM.

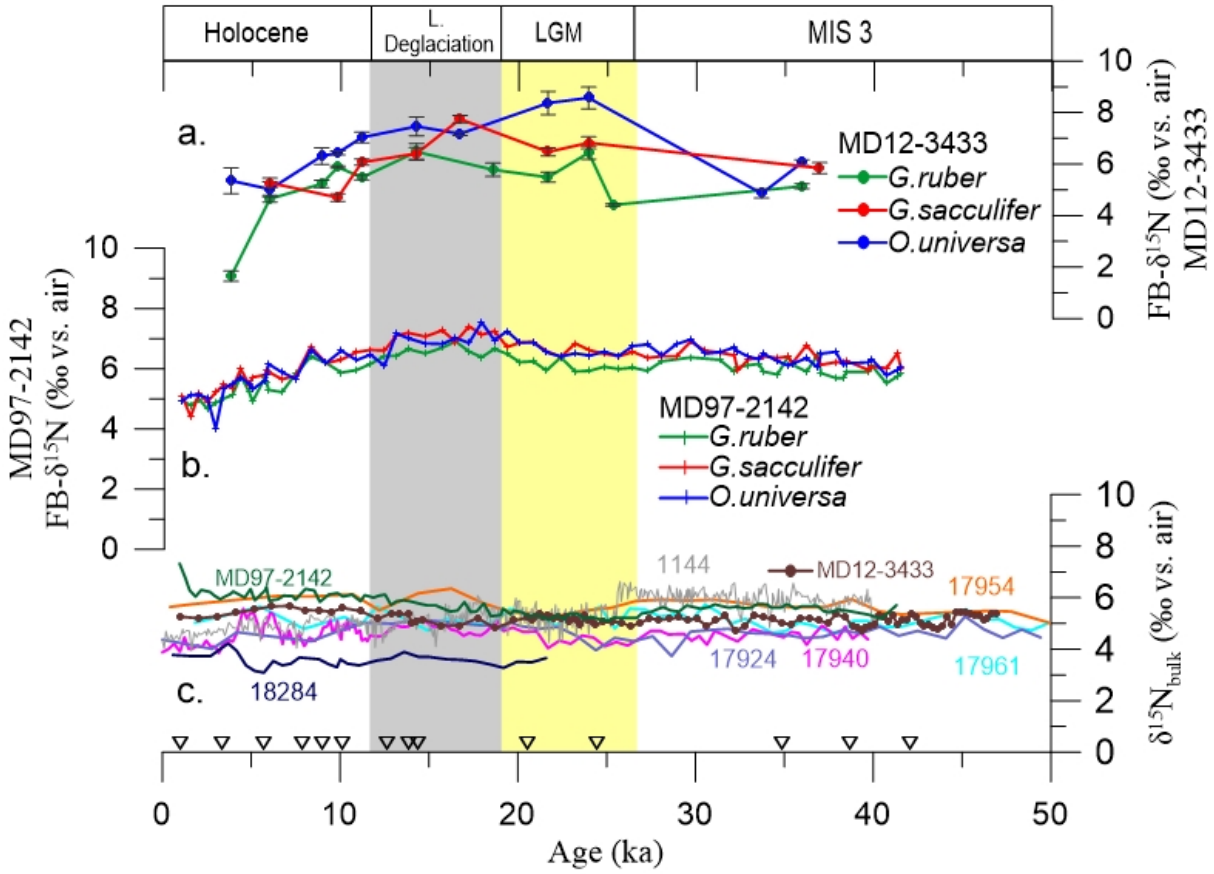

Figure 2. FB-$\delta^{15}N$ and $\delta^{15}N_{bulk}$ results of core MD12-3433, in comparison with other cores. (a) FB-$\delta^{15}N$ of *G. ruber* (green circles), *G. sacculifer* (red circles) and *O. universa* (blue circles) of core MD12-3433 in this study. (b) FB-$\delta^{15}N$ of *G. ruber* (green crosses), *G. sacculifer* (red crosses) and *O. universa* (blue crosses) of core MD97-2142 (Ren et al., 2012a). (c) $\delta^{15}N_{bulk}$ of core MD12-3433 (brown) in this study, core MD97-2142 (Ren et al., 2012a), core 17961, core 17954, core 17940, core 17924, core 18284 (Kienast, 2000) and ODP 1144 (Higginson et al., 2003). Triangles at the bottom indicate the AMS ^{14}C dates. The gray and yellow bars indicate the last deglaciation and the LGM, respectively.

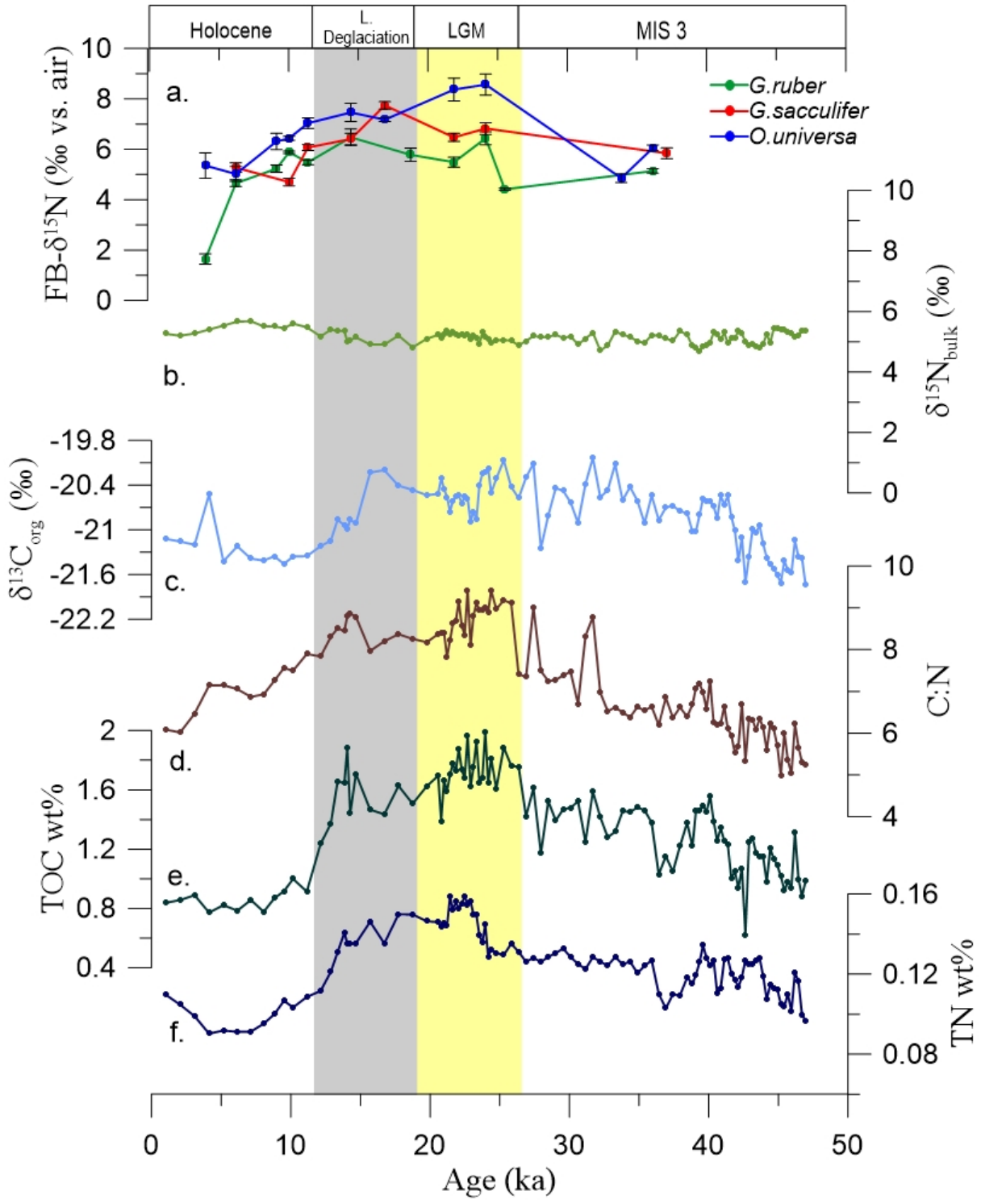

Figure 3. FB-δ^{15}N and bulk sediment records of MD12-3433. (a) FB-δ^{15}N of *G. ruber* (green

circles), *G. sacculifer* (red circles) and *O. universa* (blue circles). (b) $\delta^{15}N_{bulk}$. (c) organic $\delta^{13}C_{org}$ in sediments. (d) C:N ratios. (e) TOC weight percent %. (f) TN weight percent %. The gray and yellow bars indicate the last deglaciation and the LGM, respectively.

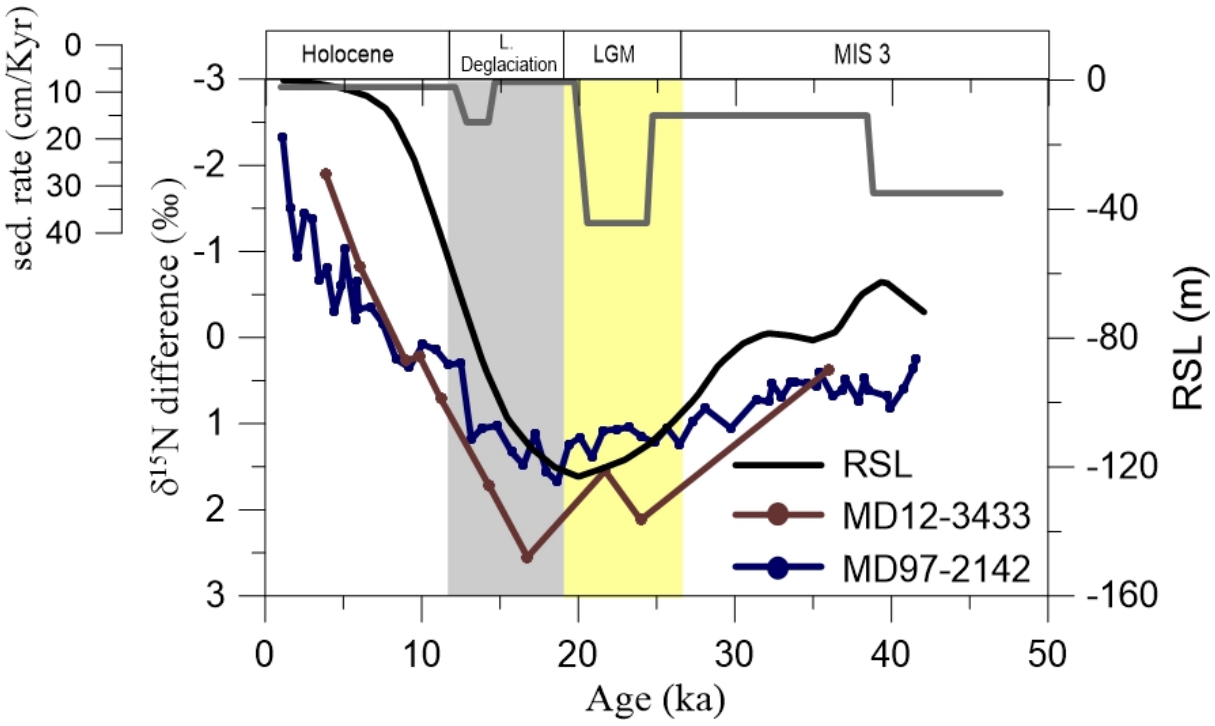

Figure 4. The comparison between relative sea level (RSL) (Waelbrocek et al., 2002) and $\delta^{15}N$ difference (FB-$\delta^{15}N$ minus $\delta^{15}N_{bulk}$) of MD12-3433 in this study and MD97-2142 (Ren et al., 2012a). Also shown is the sedimentation rate of MD12-3433 (gray line). The gray and yellow bars indicate the last deglaciation and the LGM, respectively.

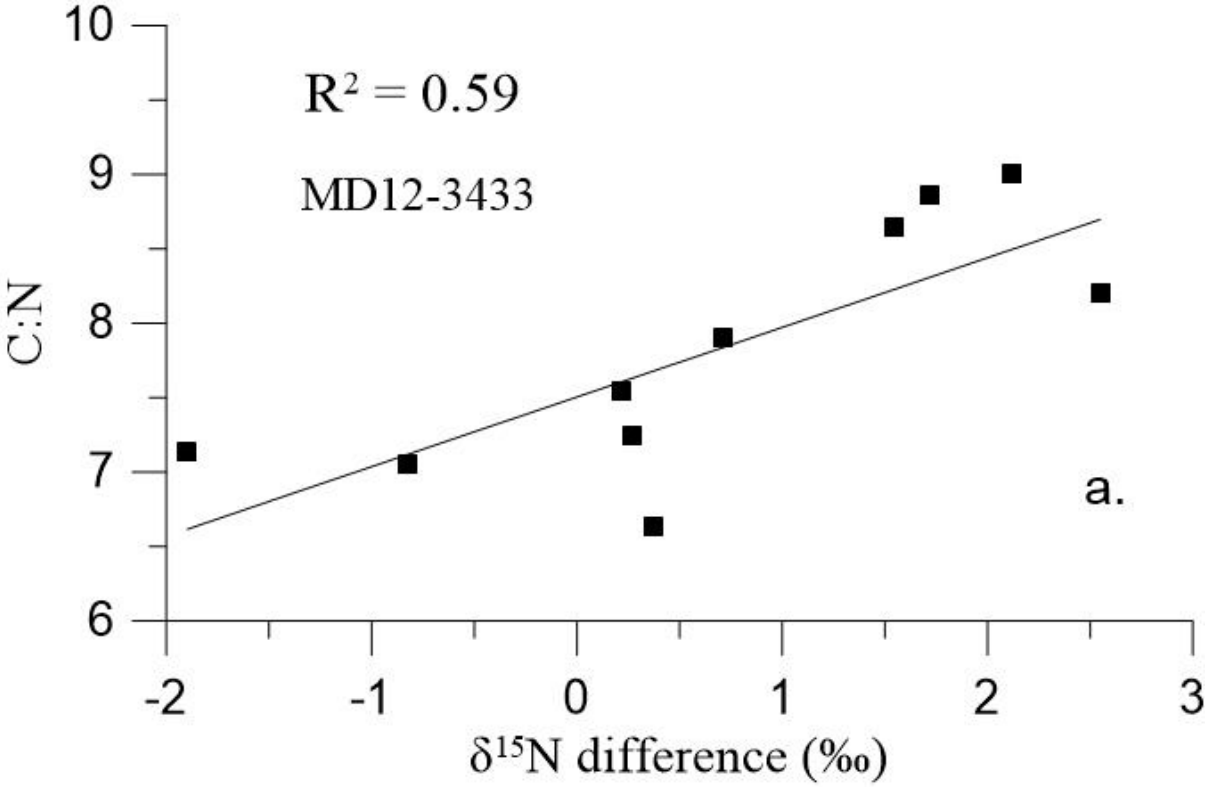

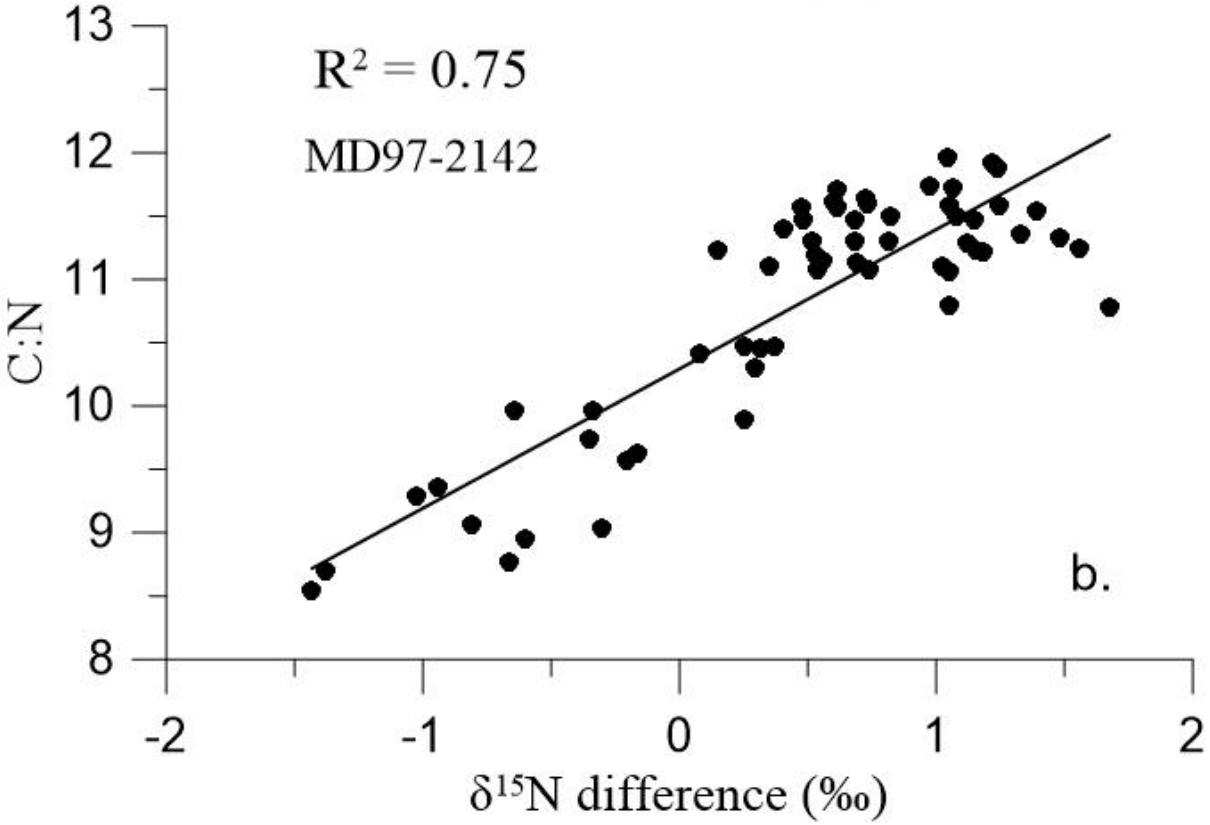

Figure 5. $\delta^{15}N$ difference (FB-$\delta^{15}N$ minus $\delta^{15}N_{bulk}$) vs. C:N for MD12-3433 (a) and MD97-2142 (Ren et al., 2012a) (b).

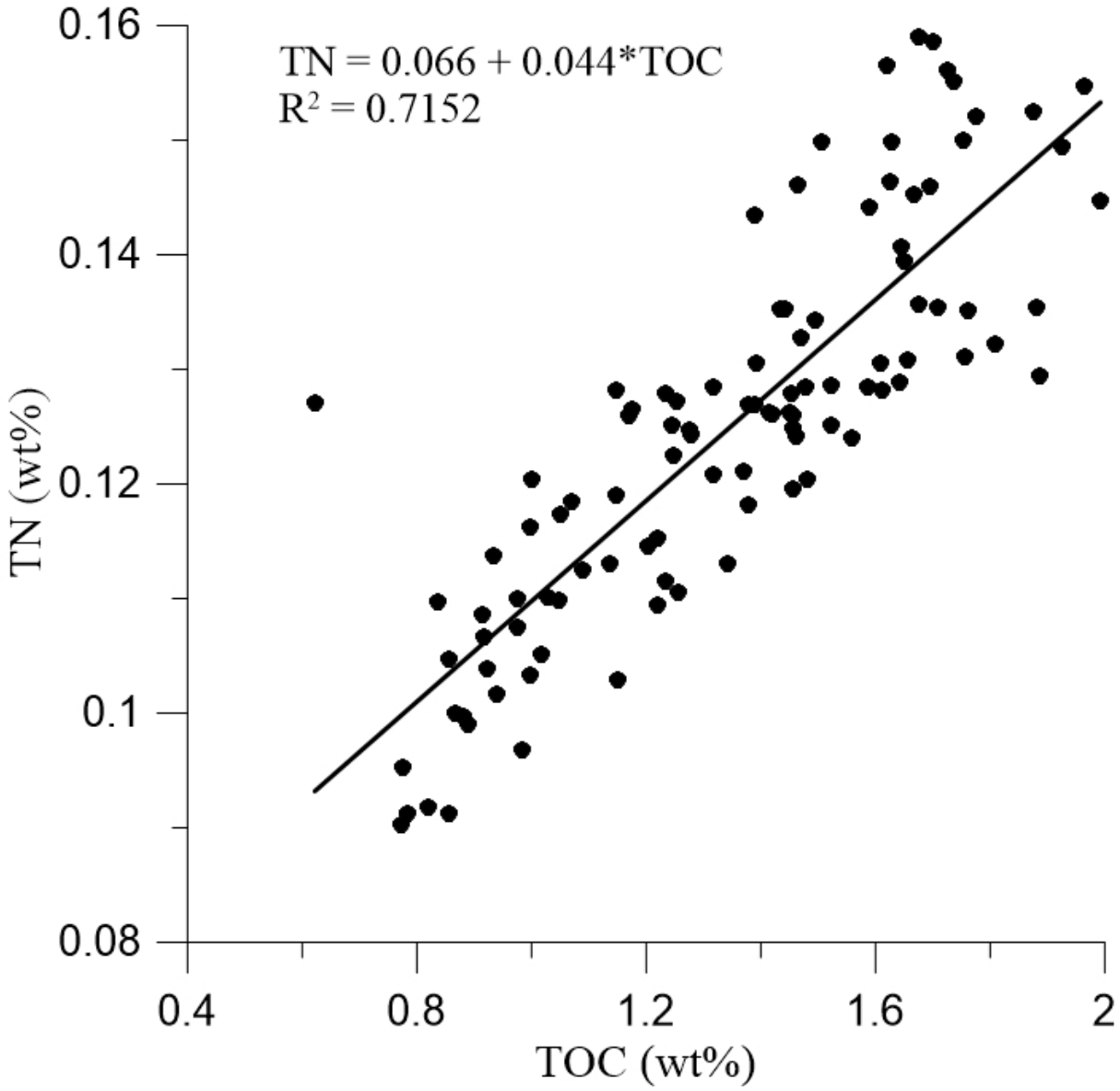

Figure 6. TOC (wt%) vs. TN (wt%) for MD12-3433. The black line is the linear relationship between TOC and TN with an intercept of 0.066, which is assumed to represent the inorganic

nitrogen fraction.

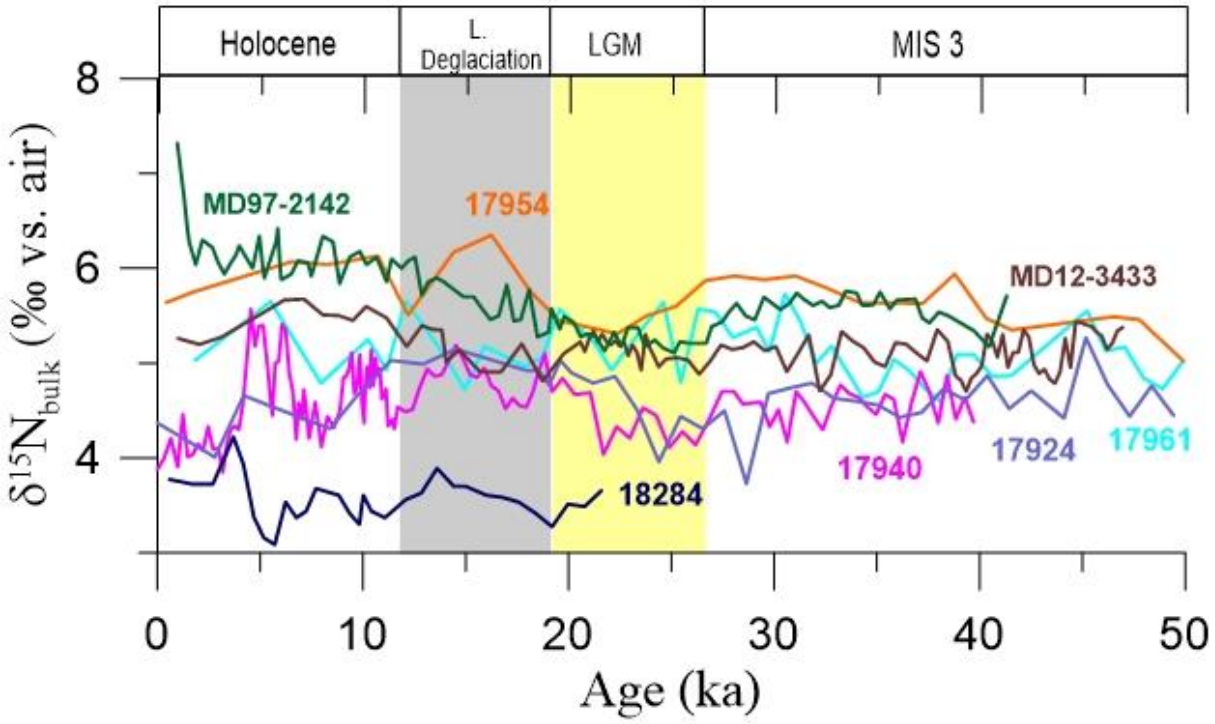

Figure 7. Seven $\delta^{15}N_{bulk}$ records all over the SCS. MD12-3433 is in this study. MD97-2142 is from (Ren et al., 2012a) and others are from (Kienast 2000). Gray and yellow bars indicate the last deglaciation and the LGM, respectively.

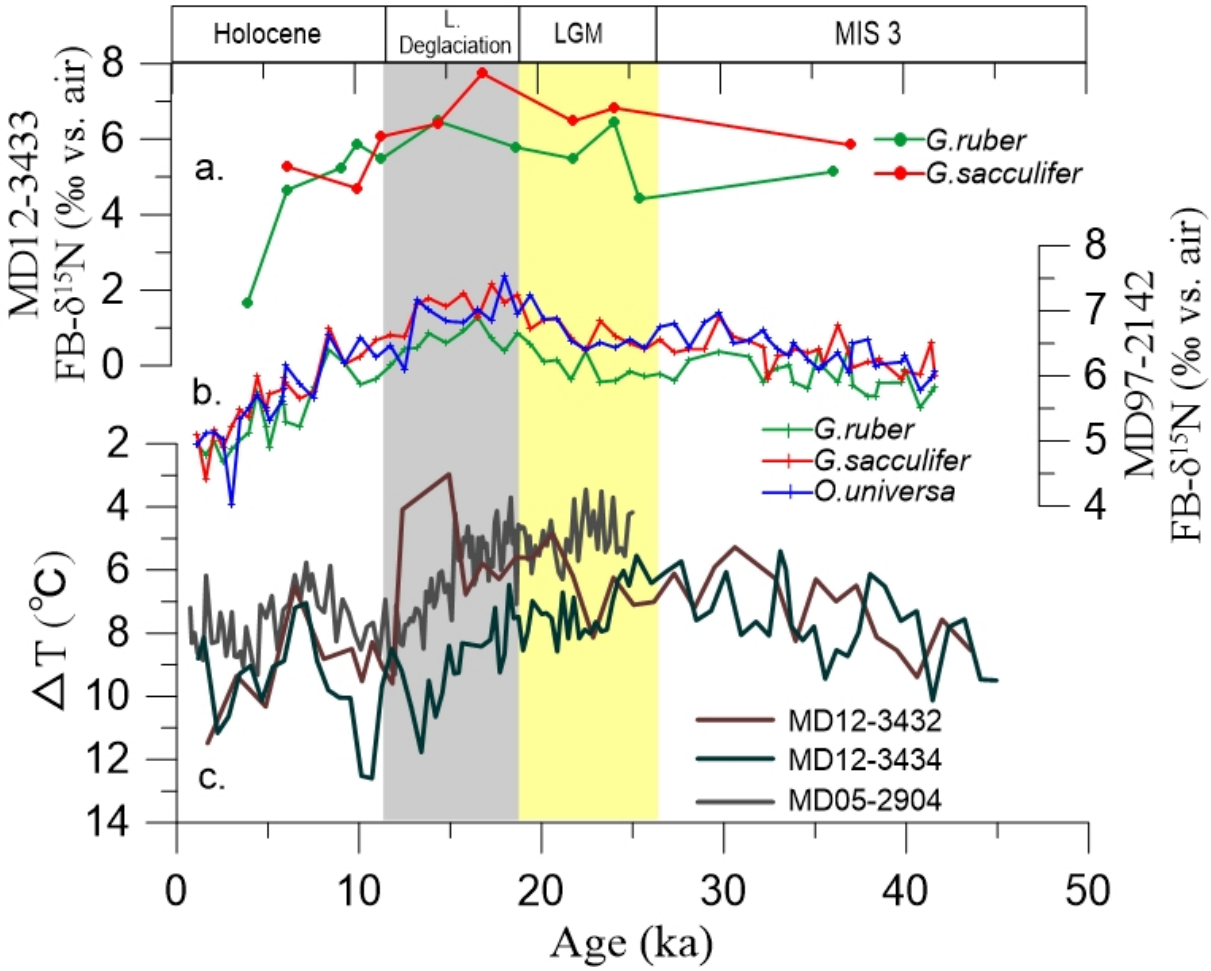

Figure 8. The comparison between FB-δ^{15}N and the seawater temperature difference between surface and thermocline (ΔT). (a) FB-δ^{15}N of *G. ruber* (green circles) and *G. sacculifer* (red circles) of core MD12-3433. (b) FB-δ^{15}N of *G. ruber* (green circles), *G. sacculifer* (red circles) and *O. universa* (blue circles) of core MD97-2142 (Ren et al., 2012a). (c) ΔT (SST-TWT) derived from Mg/Ca of *G. ruber* and *P. obliquiloculata* of core MD12-3432 (the brown line), MD12-3434 (the green line) and MD05-2904 (the gray line) (Steinke et al., 2011). Gray and yellow bars indicate the last deglaciation and the LGM, respectively.